Influence of Large-Amplitude Oscillations on Turbulent Drag

Zhuoxiong Mao and Thomas J. Hanratty
University of Illinois, Urbana, IL 61801

The effect of imposed large-amplitude oscillations on turbulent drag is studied. The system consists of water flow through a straight 5.08-cm pipe. The velocity gradient at the wall is measured with flush-mounted electrochemical mass-transfer probes. Newly developed numerical algorithms are used to analyze the probe performance in the presence of unsteady flows. Sinusoidal oscillations are at large enough frequencies, $\omega^+ = 0.0138$–0.0506, that a pseudo-steady-state approximation cannot be made. The ratio of the time-averaged velocity gradient at the wall, with and without oscillations, $\overline{S}$, varies between 1.00 and 1.03, provided flow reversal does not occur. However, two experiments in which reversed flows existed at the wall for an appreciable period of time show drag reductions of 7 and 13%.

Imposed nonsinusoidal oscillations are also studied for a period of favorable pressure gradient, about twice longer than that of unfavorable, and two sudden changes in the pressure gradient. Experiments at $Re = 9{,}700$ with T_o of 2.00, 2.45, and 3.46 s, and at $Re = 19{,}200$ with $T_o = 3.46$ give values of $\overline{S} = 1.04$–1.08. At $Re = 19{,}200$ and $T_o = 2.00$, 1.50, 1.00 s, drag reductions are 10–15%. This phenomenon could be associated with the speed with which a flow adjusts to sudden changes in the pressure gradient.

Introduction

The imposition of periodic oscillations on a turbulent fluid flowing through a duct causes periodic changes in the shear rate (or shear stress) at the wall, S. As shown by Hussain and Reynolds (1970), these changes can by characterized by defining $S(t)$ as the sum of a phase-averaged and a fluctuating quantity,

$$S(t) = \langle S(t) \rangle + s(t), \tag{1}$$

where $\langle S(t) \rangle$ may be considered as the sum of a time-average and an induced periodic variation:

$$\langle S(t) \rangle = \overline{S} + \tilde{S}(t). \tag{2}$$

The average of s^2 at a fixed phase for a large number of periods is designated as $\langle s^2 \rangle$, which also can be set equal to a time-average and a periodic variation:

$$\langle s^2 \rangle = \overline{s^2} + \tilde{s^2} \tag{3}$$

A number of studies with imposed sinusoidal oscillations of small or moderate amplitude reveal that the time average of the shear rate, $\overline{S}$, and of the turbulence, $\overline{s^2}$, is the same as what would be observed in the absence of imposed oscillations, even though large variations of the phase-averaged turbulence occur (Mao and Hanratty, 1986; Finnicum and Hanratty, 1988; Ronnenberger and Ahrens, 1977; Mizushina et al., 1973; Tu and Ramaprian, 1983; Ramaprian and Tu, 1983).

This article presents results from experiments which were carried out to determine whether the imposition of large-amplitude sinusoidal (with flow reversal at the wall) or nonsinusoidal oscillations (without flow reversal) could change the time-averaged drag at the wall. The experiments were conducted in a 5.08-cm pipeline through which an electrolyte solution was flowing turbulently. The oscillations were introduced by a plunger pump whose motion was controlled to give the desired imposed flow oscillation. A critical problem was the measurement of the drag at the wall under conditions that the amplitude of oscillation is larger than the time average.

Measurement of the Wall Shear Stress

The time-varying velocity gradient at the wall, $S(t)$, was determined by measuring the current to a pair of small electrodes, mounted flush on the wall, which are the cathodes of an electrolysis cell (Hanratty and Campbell, 1983; Hanratty, 1991). The current flowing to a single electrode, I, is related to the mass-transfer rate per unit area, N, through

$$N = I/n_e AF, \tag{4}$$

where n_e is the number of electrons involved in the reaction, A, the area and F, Faraday's constant. A mass-transfer coefficient, K, can be defined as:

$$N = K(C_B - C_W), \tag{5}$$

where C_B is the concentration of reacting species in the bulk and C_W is the concentration at the wall. At high enough applied voltages the reaction rate is fast enough that $C_W = 0$, so measurements of the current are directly proportional to the mass-transfer coefficient and to the bulk concentration.

The diffusion process is characterized by a large Schmidt number and, therefore, a very small thickness, δ_c, of the concentration boundary layer over the electrode. As a consequence, the velocity field can be represented by $\vec{u} = \vec{S}y$ where y is the distance from the surface. It has been shown by Mitchell and Hanratty (1966) that small circular electrodes or rectangular electrodes with the long side perpendicular to the direction of mean flow are sensitive only to the component of the velocity gradient in the direction of mean flow, designated as S. The mass-balance equation for the reacting species over the electrode for small δ_c and for negligible effects of diffusion in the flow direction is given by:

$$\frac{\partial C}{\partial t} + Sy\frac{\partial C}{\partial x} = D\frac{\partial^2 C}{\partial y^2}. \tag{6}$$

The solution of Eq. 6 for steady laminar flow is:

$$K = \alpha S^{1/3}, \tag{7}$$

$$\alpha = 0.807\frac{D^{2/3}}{L^{1/3}}, \tag{8}$$

where L is the length of the electrode. Consequently, the velocity gradient can be determined by measuring the electric current (or K). If the dimensions of the electrode can be carefully controlled, no calibration is necessary. The influence of diffusion in the flow direction under steady-flow conditions is related to the dimensionless group:

$$Z = \frac{SL^2}{D} = L^{+2}Sc, \tag{9}$$

where Sc is the Schmidt number and L^+ is the length of the electrode made dimensionless with respect to the kinematic viscosity, ν, and the friction velocity, v^*. Errors in Eq. 7 are less than 5% if $Z > 200$ with a rectangular electrode and if $Z > 1{,}000$ with a circular electrode.

The neglect of diffusion under unsteady-flow conditions with large enough fluctuations that the flow is reversing direction ($S \cong 0$) requires further consideration. The argument used by Kaiping (1983) is that the use of Eq. 6 is valid provided $\partial C/\partial t$ is much larger than $D(\partial^2 C/\partial x^2)$. This, in turn, requires $\omega^+ L^{+2} Sc$ is large. For our experiments, $L^{+2}Sc \cong 900$. For experiments in which flow reversal was experienced, $\omega^+ L^+ Sc = 27$ and 45, so that the use of Eq. 6 seems justified.

Equation 7 has been used for unsteady flows by assuming that the frequency is small enough that a pseudo-steady-state assumption can be made, whereby it is valid at each time, even though S varies with time. The analysis of the frequency response of electrochemical wall shear stress probes has largely focused on a flow with superimposed small-amplitude oscillations (Mitchell and Hanratty, 1966; Fortuna and Hanratty, 1971; Mao and Hanratty, 1986; Ambari et al., 1986). They show that the validity of the pseudo-steady-state approximation depends on the dimensionless group:

$$\omega^* = \omega^+ (L^{+2}Sc)^{1/3}, \tag{10}$$

where ω is the circular frequency in radians per unit time and $\omega^+ = \omega\nu/u^{*2} = \omega/S$. Errors in using the pseudo-steady approximation to analyze a small-amplitude sinusoidal current oscillation will be less than 5% in calculating the amplitude of S if $\omega^* < 2$ and less than 5° in calculating the phase if $\omega^* < 0.2$.

The analyses by Pedley (1976) and by Kaiping (1983) are much more relevant to the measurements presented here. They considered a sinusoidally varying S with no turbulence:

$$S = \bar{S} + \tilde{S} \tag{11}$$

$$\tilde{S} = \hat{S}\cos\omega t \tag{12}$$

Equation 6 was solved by finite difference methods to give the periodically varying transfer rate to a flush-mounted probe. Results from such an analysis, taken from the article by Mao and Hanratty (1991a), are presented in Figures 1 and 2. Here

$$Nu^* = \frac{KL}{D}(L^{+2}Sc)^{-1/3} \tag{13}$$

and the friction velocity used in evaluating L^+ is calculated with $\bar{S}$.

Figure 1 gives results for a large-amplitude oscillation with no flow reversal:

$$\frac{S}{\bar{S}} = 1 + 0.9\cos\omega t \tag{14}$$

It shows that the quasi-steady approximation gives inaccurate results for $\omega^* \geq 0.1$. The amplitude is overpredicted and no higher harmonics appear in the calculated Nu^*. Figure 2 gives results for a flow in which the oscillations cause reversals in the direction of S for part of the cycle:

$$\frac{S}{\bar{S}} = 1 + 2.0\cos\omega t \tag{15}$$

Here, it would be very difficult for the values of ω^* explored

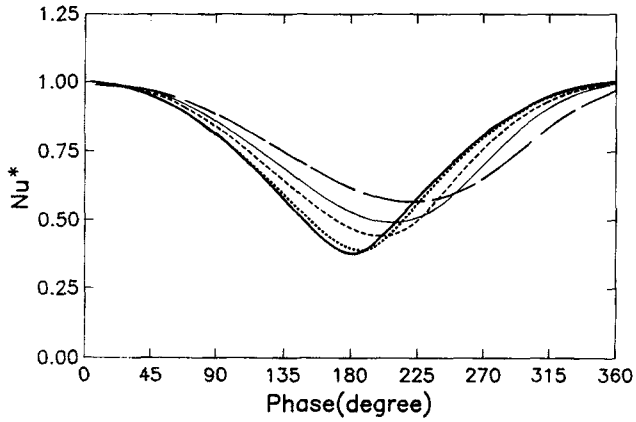

Figure 1. Numerical calculations of modified Nusselt number for shear rate $S = 1 + 0.9 \cos(\omega^* \tau)$.

—, quasi-steady solution; ····, $\omega^* = 0.1$; - - -, $\omega^* = 0.5$; —, $\omega^* = 1.0$; — —, $\omega = 2.0$.

to use the quasi-steady approximation to determine $S(t)$ from the measured $K(t)$.

Studies of the effect of large-amplitude sinusoidal oscillations with no flow reversal were initiated in this laboratory by Mathews (1987). These produced periodic $K(t)$ measurements with a significant second harmonic. An analysis of these results using the pseudo-steady-state approximation would suggest a nonlinear hydrodynamic interaction. However, a consideration of Figure 1 indicates that this interpretation could be incorrect and that the nonsinusoidal $K(t)$ could result from the time response of the wall probe to a sinusoidal flow oscillation. These considerations, in addition to the difficulties experienced in interpreting measurements of $K(t)$ with the pseudo-steady-state equation in a flow which is reversing direction, lead to the use of inverse mass-transfer techniques based on Eq. 6.

Two methods were explored by Mao and Hanratty (1991a) to interpret $K(t)$ results of the type in Figures 1 and 2. In one of these a function for $S(t)$ with several unknown parameters is assumed. An iterative scheme was developed to determine these parameters, which involved several numerical (finite difference) solutions of Eq. 6. The second method does not estimate $S(t)$ for the whole time domain. Instead, it is assumed that the $S(t)$ for $t \leq t_k$ are known and that the predicted $K(t)$ for $t \leq t_k$ are a good fit to the measurements. Then, $S(t_{k+1})$ is calculated at t_{k+1} from experimental data on K at t_{k+1} and the knowledge about $S(t)$ for $t \leq t_k$. This is accomplished by an iterative method in which S at t_{k+1} is assumed and the mass-balance equation is solved numerically to obtain K at t_{k+1}. If this agrees with the measurement, then the assumed S is correct. The application of these approaches to analyze the $K(t)$ signals in Figure 1 produced Eq. 14 for each of the curves shown. The treatment of $K(t)$ signals for reversing flows required additional information about the flow direction at each time step. The analysis of Figure 2, along with the specification of the flow direction, gave Eq. 15 for all of the curves shown.

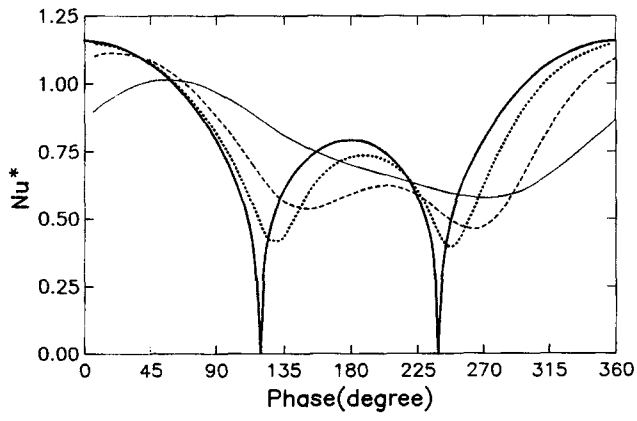

Figure 2. Numerical calculations of modified Nusselt numbers for $S = 1 + 2.0 \cos(\omega t)$.

— quasi-steady solution; ··· $\omega^* = 0.2$, - - - $\omega^* = 1.0$, — — $\omega^* = 5.0$.

The sequential estimation method outlined above was used by Mao and Hanratty (1991b) to analyze measurements made in a turbulent flow. The electrode was a circular wire with a diameter of 0.0127 cm. The measured $K(t)$ was digitized at 25,600 points and the value of $S(t)$ corresponding to each point was calculated with the numerical algorithm. This signal was analyzed to obtain the probability distribution and the frequency spectrum of $s(t)$. These gave $(\overline{s^2})^{1/2} = 0.37\ \overline{S}$, a skewness of 0.96 and a flatness of 4.2. A comparison of the frequency spectra obtained using linear and nonlinear analyses reveals that the linear theory correction underestimates the energy content of the large-amplitude high-frequency fluctuations that exist in a turbulent flow.

Mass-transfer measurements to a single probe cannot determine the time-averaged velocity gradient when imposed oscillations in the flow are large enough to cause flow reversal since knowledge about the instantaneous flow direction is needed. One approach that seems attractive is to use two identical rectangular electrodes separated by a thin layer of insulation. The sign of the difference in the mass-transfer rates, N_1-N_2, has been suggested by Son and Hanratty (1969) and by Py (1973) as directly related to flow direction. Finite difference solutions of Eq. 6 for such an arrangement show, for large enough ω^*, that a change in the sign of K_1-K_2 is not coincident with a change in the direction S. This led Mao and Hanratty (1991c) to consider in detail the frequency response of a sandwich electrode. On the basis of these calculations, they suggested an inverse mass-transfer analysis of measurements of N_1-N_2 that could determine $S(t)$ both in reversing and nonreversing conditions.

The Experiments

The electrochemical techniques used in this study are described in review articles by Hanratty and Campbell (1983) and Hanratty (1991). A solution that was 0.1 molar in potassium iodide and 1.5×10^{-3} molar in iodine was circulated through a 5-cm pipe by a centrifugal pump. The temperature of the solution was controlled at 25 ± 0.1 °C and the flow rate was measured with a magnetic flowmeter. The kinematic viscosity of the solution was 0.0085 cm^2/s and the Schmidt number, Sc, characterizing the diffusing species was 850.

Sinusoidal flow oscillations were introduced by a reciprocating plunger pump with an adjustable stroke length. The frequency was controlled by changing the voltage applied to the DC motor used to drive the plunger.

Nonsinusoidal oscillations were introduced by using a specially designed cam to drive the plunger pump. The radius of the cam is a function of θ. When the cam is driven by a DC motor, the velocity of the plunger is described as:

$$u(t)=\frac{dr(\theta)}{dt} \tag{16}$$

where θ equals $\omega_o t$. For a prescribed $u(t)$, the shape of the cam is determined by integrating Eq. 16.

A C.J. Enterprises differential pressure transmitter was used to determine the time-varying pressure gradient in the test section. The transmitter was calibrated by closing off the main pump so that only flow pulsations were transmitted down the pipe. Because of the incompressibility of the fluid, the motion in the test section was in phase with the piston and the oscillating pressure gradient could be calculated from the piston stroke length. This calibration procedure is described by Mao and Hanratty (1986) and by Finnicum and Hanratty (1988) and in theses by Mao (1984) and Finnicum (1986). Calibration curves by Finnicum (1986) show that the amplitude response of the transducers is flat over all frequencies.

The oscillations in the centerline velocity were not measured, but calculated from the measured fluctuations in the pressure gradient by using

$$\rho\frac{dU_c}{dt}=-\frac{\partial p}{\partial x} \tag{17}$$

This gives a centerline velocity that lags variations in the favorable pressure gradient by 90° with the magnitude of

$$|\tilde{U}_c|=-\frac{1}{\rho\omega}\left|\frac{d\tilde{p}}{dx}\right|. \tag{18}$$

The accuracy of using Eq. 18 is explained in detail by Finnicum and Hanratty (1988).

The reactions that occurred at the two electrodes are:

$$\text{Cathode}\quad I_3^- + 2e \rightarrow 3I^-$$
$$\text{Anode}\quad 3I^- \rightarrow I_3^- + 2e$$

The anode, which was a section of stainless steel pipe, had a much larger area than the cathode so the current was controlled by the reaction at the cathode.

The sandwich probes used as cathodes were made from two pieces of 0.0102-cm platinum sheet and teflon tape. The platinum sheets and the teflon tape were glued together with epoxy under pressure. The probe was inserted into a plexiglass block. One end of the block was sanded with sand paper and then polished with magnesium oxide powder. The block was glued in a hole in the test section so that the surface of the block was flush with the internal wall of the pipe. The actual dimensions of the probe were measured from a magnified photograph of 0.011×0.093 cm for each electrode and as 0.0024 cm for the insulation between the electrodes, so that the ratio of the insulation thickness to electrode length, γ_i, was 0.22. The measured electrode sizes were checked by comparing the time-averaged electric current to each of the electrodes (operating separately) when no oscillations were introduced. No differences were noted so no corrections had to be introduced because the electrodes had unequal size.

The electrochemical technique and the electric circuit used to obtain voltage outputs (proportional to the current) from the two cathodes are described by Hanratty and Campbell (1983). The voltage signals from the two electrodes were digitized by a 12-bit A/D converter and sampled in two separate channels by an LSI/11 minicomputer manufactured by Digital Equipment Corporation. An optio-interrupter on the plunger pump provided a trigger signal to start sampling the data when the plunger reached a certain position. In each experiment, 500 periods with 64 points for each period were sampled.

The experimental conditions for the experiments with imposed sinusoidal conditions are listed in Table 1. For all of the runs, the dimensionless length and width of the electrodes were $L^+=1.03$ and $W^+=8.7$. The dimensionless group $L^{+2}Sc$ had a value of 880–910. The discussion after Eq. 9 revealed that this is large enough that molecular diffusion in the flow direction was not important under steady flow conditions.

Equation 7 can be rewritten as

$$\frac{KL}{D}=0.807\,(L^{+2}Sc)^{1/3}. \tag{19}$$

If a thickness of the concentration boundary layer is defined as $\delta_c=D/K$, then the following relation is obtained for δ_c:

$$0.807\,\delta_c^+=(L^+/Sc)^{1/3}. \tag{20}$$

In the experiments, it is desired that δ_c^+ be less than the thickness of the viscous wall region and the Stokes layer in order for Eq. 6 to be valid. For the frequencies studied, the Stokes layer varies from 6.3–12 wall units. Consequently, the requirement that $\delta_c^+<5$ is sufficient to insure that the concentration boundary layer is thinner than both the viscous wall region and the Stokes layer. For the conditions in Table 1, $L^+/Sc=1.2\times10^{-3}$, so that $\delta_c^+=0.13$.

Table 1. Time-Averaged and Phase-Averaged Data for Experiments with Imposed Sinusoidal Oscillation

				Time, Mean		Phase, Average		
ω^+	Re	u^* (cm/s)	$\hat{U}_c/\overline{U}_c$	$\overline{S}$	$\sqrt{\overline{S^2}}/\overline{S}$	$\hat{S}/\overline{S}$	ϕ	$(\hat{S}/S)/(\hat{U}_c/u^*)$
0.0138	10690	0.801	0.190	1.01	0.34	0.36	43.5	0.095
0.0138	10660	0.799	0.264	1.00	0.39	0.57	42.9	0.108
0.0276	10590	0.801	0.206	1.03	0.39	0.77	50.0	0.186
0.0276	10580	0.795	0.384	0.95	0.39	1.34	54.0	0.175
0.0506	10500	0.785	0.192	1.02	0.41	1.05	65.3	0.274
0.0506	10610	0.797	0.377	0.89	0.46	1.92	63.4	0.254

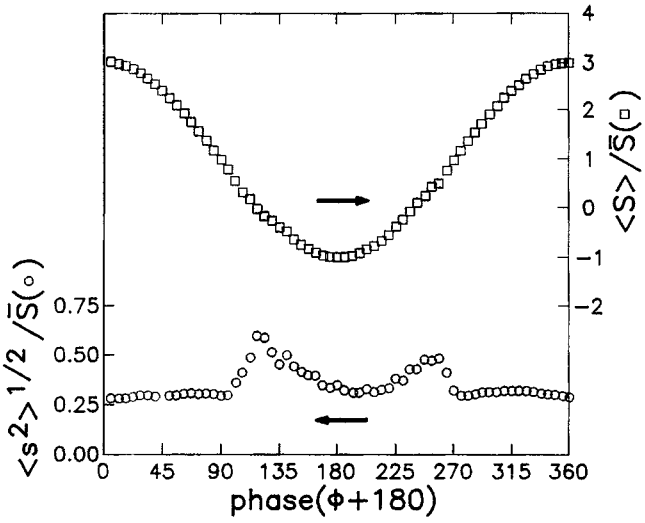

Figure 3. Numerical experiment for $\omega^+ = 0.0502$, $\bar{S} = 0.997$, $(\bar{s^2})^{1/2} = 0.363$.

The values of ω^* calculated for the runs in Table 1 are 0.13 for $\omega^+ = 0.0138$, 0.27 for $\omega^+ = 0.0276$, and 0.49 for $\omega^+ = 0.0506$. Figures 1 and 2 show that the use of a pseudo-steady-state approximation would not be valid for the experiments performed.

Test of Method of Analysis

Results in previous articles have shown that the inverse analysis can be used to obtain accurate measurements of the time mean and fluctuations of S in the presence of large-amplitude oscillations. Its applicability when flow reversals occur at the wall has not been firmly established. Therefore, a numerical test was carried out.

A set of digitized data representative of turbulent fluctuations, $s(t)$, at $Re = 10{,}500$ for a flow with no imposed flow oscillation was used. A time-varying signal given by $S = 1 + 2\cos\omega t$, with $\omega^+ = 0.0506$, was added to these data. The resulting digitized data represented a turbulent flow with reversal over part of the cycle and with $\bar{S} = 1.0$. Equation 6 was used to calculate $K(t)$ from the data.

The inverse mass-transfer method was then used to determine $S(t)$ from $K(t)$. This gave the $\langle S\rangle$ and $\langle s^2\rangle^{1/2}$ in Figure 3. Large values of $\langle s^2\rangle^{1/2}$ are noted at locations where $\langle S\rangle$ changes sign. However, if these large values are ignored, no significant differences in $\langle s^2\rangle^{1/2}$ were found in the forward and reversing flows. Of most interest, from the viewpoint of our goals, is the calculation of $\bar{S} = 0.997$.

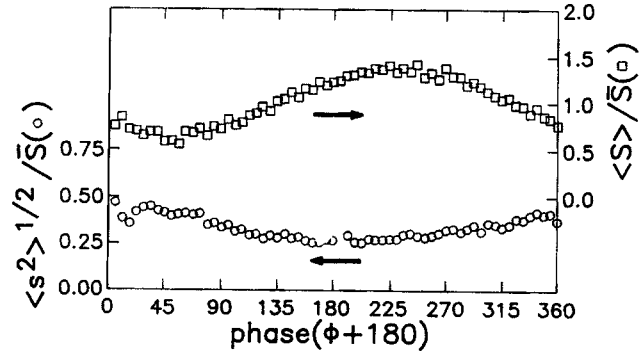

Figure 4. Phase average of s^2 and S for $\omega^+ = 0.0138$, $\hat{U}_c/\bar{U}_c = 0.190$, $Re = 10{,}690$; $\bar{S} = 1.01$, $(\bar{s^2})^{1/2} = 0.34$.

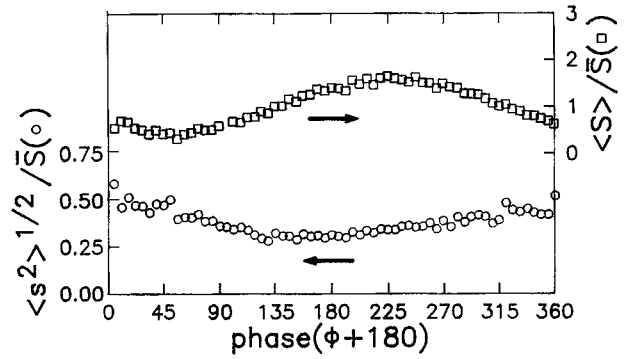

Figure 5. Phase average of s^2 and S for $\omega^+ = 0.0138$, $\hat{U}_c/\bar{U}_c = 0.264$, $Re = 10{,}660$; $\bar{S} = 1.00$, $(\bar{s^2})^{1/2} = 0.39$.

From this experiment and work decribed in previous articles, one concludes that the inverse method developed by Mao can accurately determine $\bar{S}$ in the presence of reversing flows if Eq. 6 correctly represents the concentration field. Measurements of $\langle s^2\rangle$ can be obtained only if the flow at the wall does not change direction.

However, as pointed out by Mao and Hanratty (1991c), it is possible to improve the numerical algorithm. More iterations and a stricter criterion for convergence in regions where S is a changing sign could be used. Furthermore, the measurement of $(Nu_1 + Nu_2)$ in addition to $(Nu_1 - Nu_2)$ could be beneficial.

Results with Sinusoidal Oscillations

No flow reversal

Three runs were carried out with imposed sinusoidal flow oscillations which were large, but not enough to cause flow reversals at the wall. These were done for $\omega^+ = 0.0138$ with $\hat{U}_c/\bar{U}_c = 0.190$, 0.264 and for $\omega^+ = 0.0276$ with $\hat{U}_c/\bar{U}_c = 0.206$, where $\hat{U}_c$ is the amplitude of the induced flow oscillation and U_c is the time-averaged velocity at the center of the pipe. The conditions for these runs are given in Table 1. Figures 4, 5 and 6 present phase-averaged values of S and of s^2 as a function of the phase angle, relative to the centerline velocity:

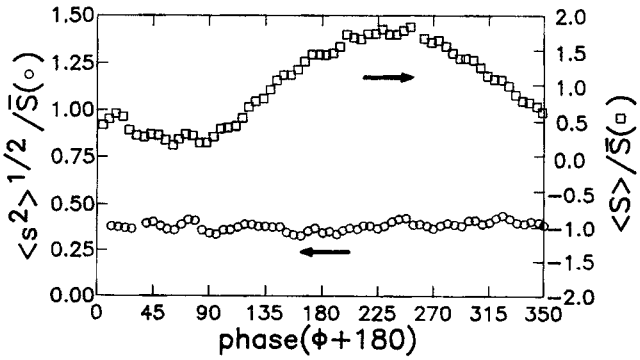

Figure 6. Phase average of s^2 and S for $\omega^+ = 0.0276$, $\hat{U}_c/\bar{U}_c = 0.206$, $\bar{S} = 1.03$, $(\bar{s^2})^{1/2}/\bar{S} = 0.39$.

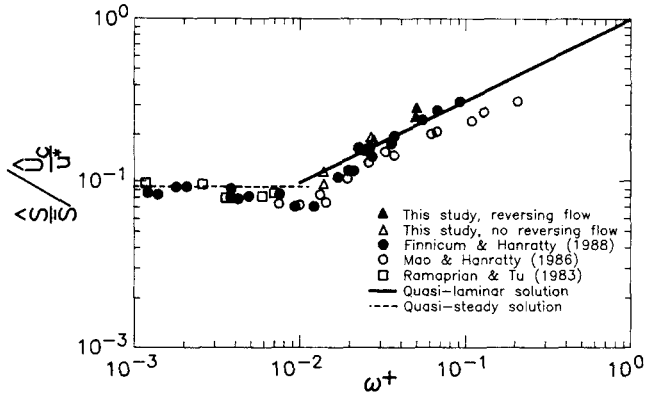

Figure 7. Amplitude of variations of the phase-averaged velocity gradient for small and large variations of the centerline velocity.

$$\langle U_c \rangle = \overline{U}_c + \hat{U}_c \cos \omega t. \tag{21}$$

The measurements of $\langle S \rangle$ and $\langle s^2 \rangle^{1/2}$ are made dimensionless with $\overline{S}$, determined in the absence of imposed oscillations.

The results on $\langle S \rangle$ are fitted with a single harmonic:

$$\langle S \rangle = \overline{S} + \hat{S} \cos(\omega t + \phi), \tag{22}$$

where ϕ is the phase angle by which $\langle S \rangle$ leads U_c. It is noted from Table 1 that measured $\overline{S}$ of 1.01, 1.00, and 1.03 are obtained. An average value of 1.01 and possible error of $\pm 2\%$ is indicated. These correspond to amplitudes $\hat{S}$ of 0.36, 0.57, and 0.77. Values of the ratio of $\hat{S}$ (made dimensionless with $\overline{S}$) to $\overline{u_c}$ (made dimensionless with the friction velocity) are also given in Table 1. This ratio and the phase angle are close to what would be calculated with linear theory using a quasi-laminar approximation (Mao and Hanratty, 1986; Finnicum and Hanratty, 1988). As can be seen in Figures 7 and 8, the results in Table 1 show slightly larger $\hat{S}$ and ϕ than the measurements of Finnicum and Hanratty (1988) with very small imposed oscillations.

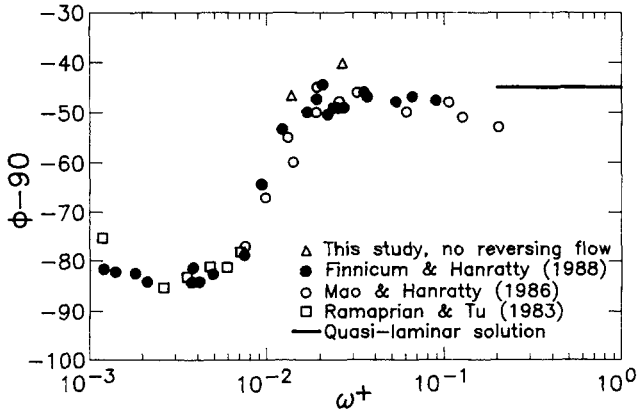

Figure 8. Phase angle variations of the phase-averaged velocity gradient for small and large variations of the centerline velocity.

ϕ is the phase lag relative to pressure gradient.

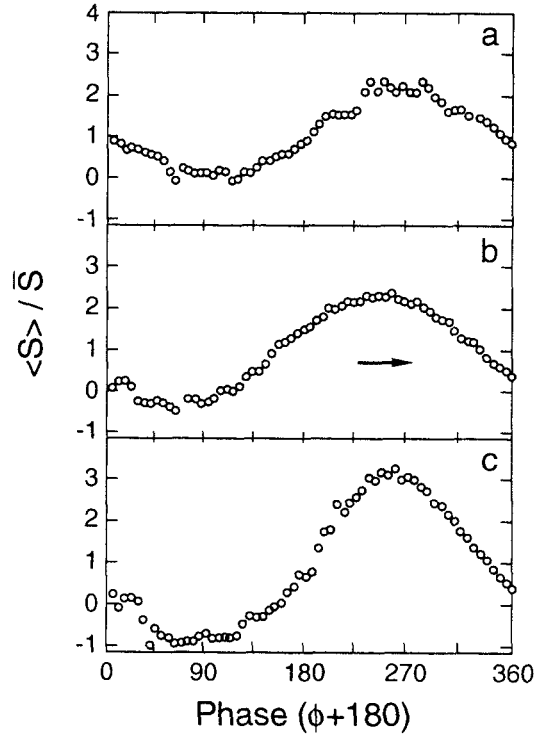

Figure 9. Phase average of S for: (a) $\omega^+ = 0.0506$, $\hat{U}_c/\overline{U}_c = 0.192$, $\overline{S} = 1.02$; (b) $\omega^+ = 0.0276$, $\hat{U}_c/\overline{U}_c = 0.384$, $\overline{S} = 0.95$; (c) $\omega^+ = 0.0506$, $\hat{U}_c/\overline{U}_c = 0.377$, $\overline{S} = 0.89$.

The measurements of $\langle s^2 \rangle^{1/2}$ at $\omega^+ = 0.0138$ show a large variation with changing phase. It is of interest to note in Figures 4 and 5 that the amplitude and phase characterizing the variation of $\langle s^2 \rangle^{1/2}$ do not change dramatically with an increase in the amplitude of the imposed oscillations. For low enough ω^+ that a pseudo-steady-state exists, phase angles of $\langle S \rangle$ and of $\langle s^2 \rangle$ are the same. As ω^+ increases, $\langle s^2 \rangle$ decreases in magnitude and lags $\langle S \rangle$. It is noted at $\omega^+ = 0.0276$ that $\langle s^2 \rangle$ shows little variation with phase. These results were obtained by Finnicum and Hanratty (1988) in their studies with small-amplitude oscillations, $\hat{U}_c/\overline{U}_c = 0.1$. For example, Finnicum found at $\omega^+ = 0.0138$ that $\langle s^2 \rangle^{1/2}$ lags $\overline{S}$ by about 75° and that the amplitude characterizing the variation of $\langle s^2 \rangle^{1/2}/\overline{S}$ changes from 0.065 to a value close to zero as ω^+ changes from 0.004 to $\omega^+ = 0.03$.

Measured values of $(\overline{s^2})^{1/2}$ of 0.34, 0.39 and 0.39 are quite close to the value of 0.37 determined by Mao and Hanratty (1991b) in the absence of imposed oscillations.

Experiments with flow reversals

As shown in Table 1, flow reversal at the wall was observed for $\omega^+ = 0.0276$, $\hat{U}_c/\overline{U}_c = 0.384$ and for $\omega^+ = 0.0506$, $\hat{U}_c/\overline{U}_c = 0.192$, 0.377. Drag reductions outside the range of experimental error were found for the two situations in which flow reversal was observed over an appreciable portion of the cycle. Drag is defined in terms of the average force on the walls in the plus direction. Thus, negative contributions are made during periods when the flow at the wall is in the negative direction.

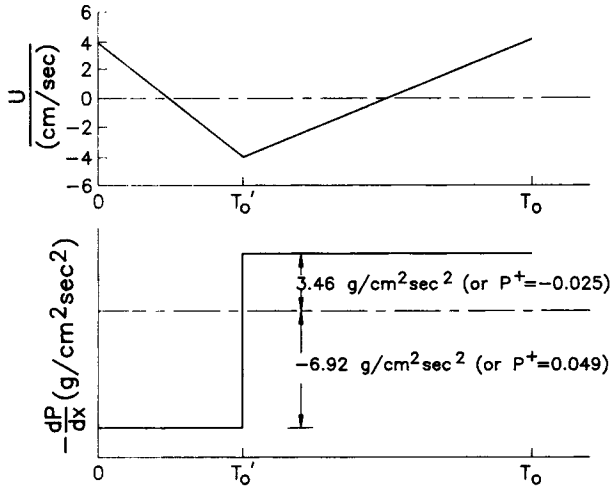

Figure 10. Idealized nonsinusoidal imposed flow oscillation.

The time variations of $\langle S \rangle$ for these experiments are shown in Figure 9. These can be fitted, approximately, with single harmonics whose amplitudes and phases are given in Table 1. As seen in Figure 7, the amplitudes agree with linear theory and with the measurements of Finnicum and Hanratty (1988) that were obtained with small-amplitude imposed oscillations. However, the phase angle is somewhat larger than $\phi = 45°$ obtained with linear theory and the studies with imposed small-amplitude oscillations.

Of particular interest in these runs is the measurement of values of $\bar{S}$ less than unity.

Results with Nonsinusoidal Oscillations

Design of the experiments

The imposed nonsinusoidal flow oscillation selected for the experiments is shown in Figure 10. The oscillating bulk velocity for one period is described as:

$$\tilde{U} = \begin{cases} -\alpha t + A & 0 \le t \le T_o' \\ \beta(t - T_o') - A & T_o' \le t \le T_o \end{cases} \tag{23}$$

This represents two ramp functions for which the period associated with the flow acceleration is twice as long as the period associated with flow deceleration. From the inviscid momentum balance, this flow corresponds to a period with a constant unfavorable pressure gradient followed by a longer period of favorable pressure gradient.

The design of the experiments was motivated by the finding (Finnicum and Hanratty, 1988; Moretti and Kays, 1965; Back and Seban, 1967; Jones and Launder, 1972; Badri Narayanan and Ramjee, 1969) that drag reduction (and even laminarization) can occur in flows with large favorable pressure gradient. A parameter representing this effect is:

$$P^+ = \frac{\nu}{\rho u^{*3}} \frac{dP}{dx}. \tag{24}$$

It is found that laminarization occurs for $P^+ \le -0.02$ to -0.025. The notion (perhaps, naive) used in designing the experiments was to explore the possibility of obtaining drag reduction by exposing the flow to a large favorable pressure gradient over 2/3 of the cycle and to an unfavorable pressure gradient over 1/3 of the cycle.

A second consideration in the design of the experiments was that the boundary layer associated with the sudden pressure changes was thick enough to obtain an interaction with the outer flow turbulence. For a laminar flow, the Stokes layer created by a step change in the pressure gradient (as opposed to a sinusoidal variation) is given as:

$$\delta_s = 4\sqrt{\nu \Delta t}. \tag{25}$$

The duration of the favorable pressure gradient, Δt, was selected so that $\delta_s^+ > 40$. For a Reynolds number of 10,000, the cam used in the experiments caused an imposed favorable pressure gradient of $P^+ = -0.02$ if a cycle time, T_o, of 2.31 s was used. The thickness of the Stokes layer at the end of accelerating phase of the cycle would be $\delta_s^+ = 73$.

Results

The conditions for the studies with nonsinusoidal oscillations are given in Table 2. Three experiments with $Re \cong 9{,}700$ and four experiments with $Re = 19{,}200$ were carried out under conditions that no flow reversal occurred. These results are plotted in Figures 11-17. Measurements are presented of $\langle S \rangle$ and of $\langle s^2 \rangle^{1/2}$ made dimensionless with the value of $\bar{S}$ determined for a flow without imposed flow oscillations. It should be noted for the experiments at $Re \cong 9{,}700$ that, during the accelerating phase, $P^+ \le -0.025$.

Furthermore, δ_s^+ characterizing these studies was large enough that $\langle S \rangle$ might be roughly given by a pseudo-steady-state approximation. The use of this approximation for a flow with imposed sinusoidal oscillations has been shown by Tu and Ramprian (1983) to give a larger time-averaged wall shear than would be calculated from the time-averaged bulk velocity

Table 2. Conditions for Experiments with Imposed Nonsinusoidal Oscillations

Re	u^* cm/s	T_0 (s)	P^+	δ_S^+	$\bar{S}$	$\sqrt{\bar{S}^2}/\bar{S}$
9,700	0.737	3.46	−0.025 ~ 0.049	70 ~ 49	1.04	0.41
9,700	0.737	2.45	−0.049 ~ 0.099	59 ~ 42	1.06	0.42
9,700	0.737	2.00	−0.074 ~ 0.148	53 ~ 38	1.08	0.42
19,200	1.338	3.46	−0.0039 ~ 0.0078	129 ~ 91	1.07	0.45
19,410	1.353	2.00	−0.012 ~ 0.024	97 ~ 69	0.91	0.41
19,400	1.352	1.50	−0.021 ~ 0.042	84 ~ 60	0.95	0.42
19,300	1.345	1.00	−0.047 ~ 0.094	69 ~ 49	0.94	0.41

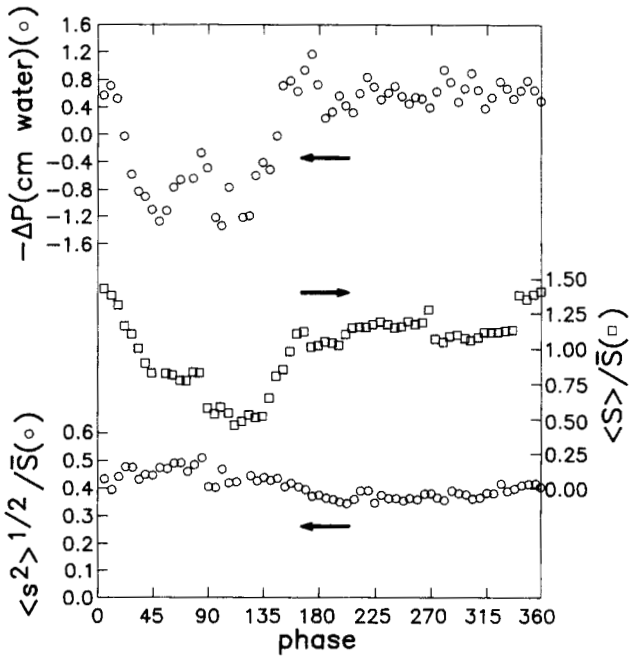

Figure 11. Results from experiment with nonsinusoidal oscillation: $Re = 9{,}700$, $T_o = 3.46$ s; $\bar{S} = 1.04$, $(\overline{s^2})^{1/2} = 0.41$.

(because of the nearly quadratic relation between wall shear stress and bulk velocity). For example, they calculated $\bar{S} = 1.01$ and 1.15 for imposed sinusoidal oscillations with $\hat{U}_c/\bar{U} = 0.15$ and 0.64. From these considerations, it is expected that the measured $\bar{S}$ with imposed nonsinusoidal oscillations should be greater than unity.

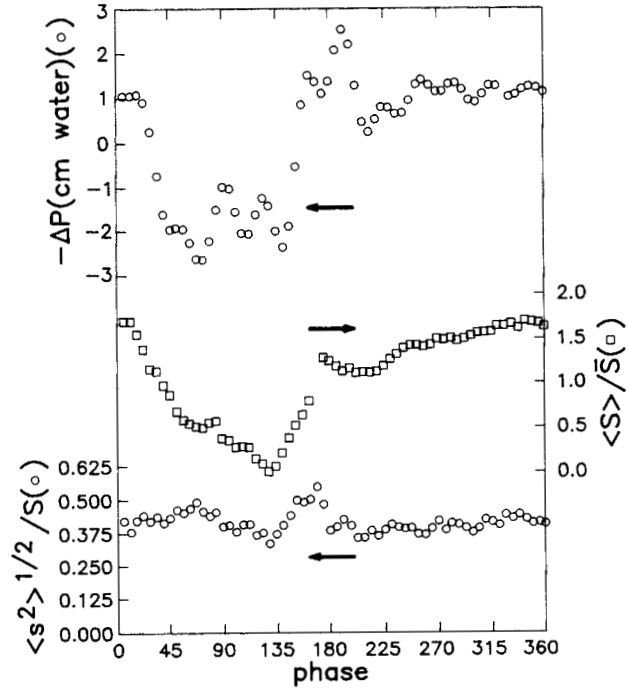

Figure 12. Results from experiment with nonsinusoidal oscillation: $Re = 9{,}740$, $T_o = 2.45$ s; $\bar{S} = 1.06$, $(\overline{s^2})^{1/2} = 0.42$.

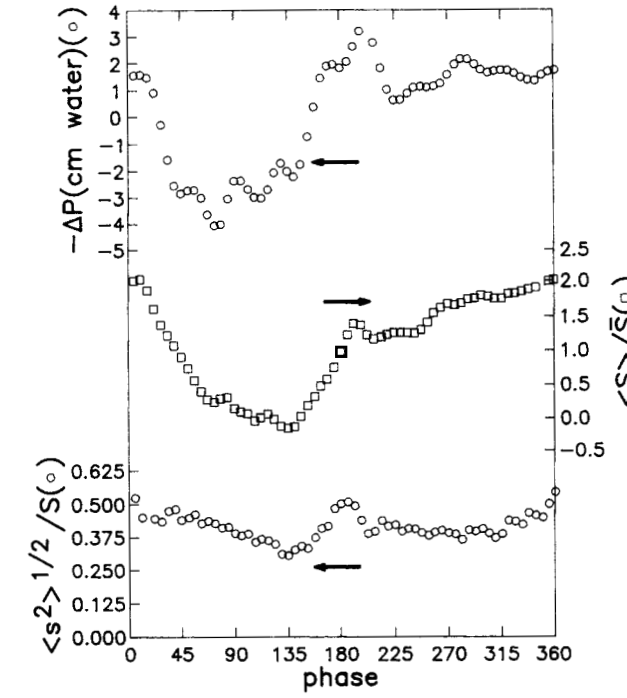

Figure 13. Results from experiment with nonsinusoidal oscillation: $Re = 9{,}700$, $T_o = 2.00$ s; $\bar{S} = 1.08$, $(\overline{s^2})^{1/2} = 0.42$.

As seen in Figures 11-17, approximately constant favorable and unfavorable pressure gradients existed, respectively, for t/T_o of 0.4 to 1.0 and for t/T_o of 0.1 to 0.3. The change from a favorable to an unfavorable pressure gradient occurs for $t/T_o = 0$ to 0.1; the change from an unfavorable to a favorable pressure gradient occurs for $t/T_o = 0.3$ to 0.4. No evidence of laminarization or of a decrease in drag during the period of favorable pressure gradient was found, so that the notion on which the experiment was based is not realized. In fact, it is found that $\bar{S}$ was greater than unity for all of the experiments at $Re = 9{,}700$ under consideration, $\bar{S} = 1.04$ to 1.08.

For the run at $Re = 9{,}700$, $T_o = 3.46$ s, the measured $\langle s^2 \rangle^{1/2}$ is larger during periods of flow deceleration than during flow

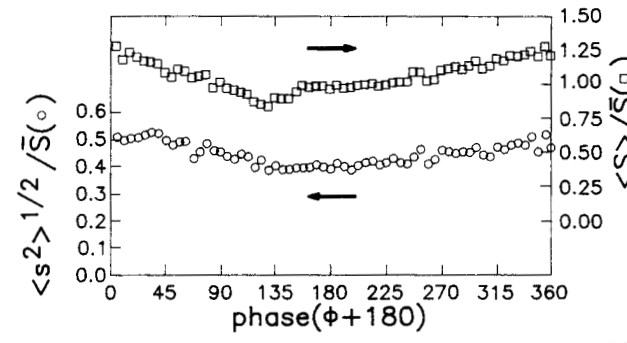

Figure 14. Results from experiment with nonsinusoidal oscillation: $Re = 19{,}200$, $T_o = 3.46$ s; $\bar{S} = 1.07$, $(\overline{s^2})^{1/2} = 0.45$.

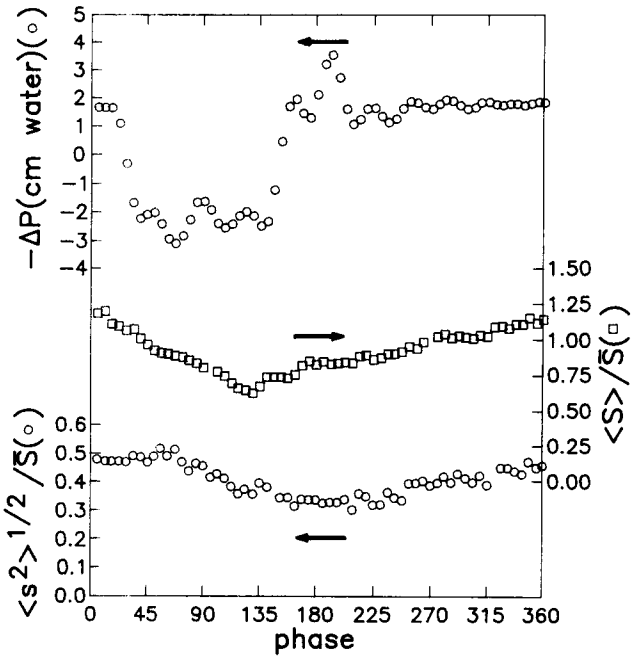

Figure 15. Results from experiment with nonsinusoidal oscillation: $Re = 19{,}410$, $T_o = 2$ s; $\bar{S} = 0.91$, $(\bar{s^2})^{1/2} = 0.41$.

acceleration. The measurements of $\langle s^2 \rangle^{1/2}$ at $Re = 9{,}700$ for $T_o = 2.45$ s and $T_o = 2.00$ s have a different behavior. Both show a sharp peak at $T_o \equiv 0.50$. This is probably associated with the overshoot in the pressure gradient at the location where the flow is adjusting to a region of constant favorable pressure gradient.

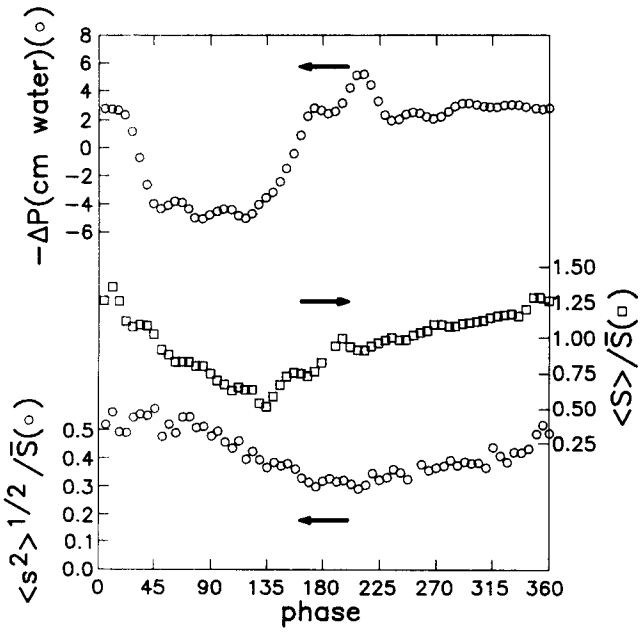

Figure 16. Results from experiment with nonsinusoidal oscillation: $Re = 19{,}300$, $T_o = 1.50$ s; $\bar{S} = 0.95$, $(\bar{s^2})^{1/2} = 0.42$.

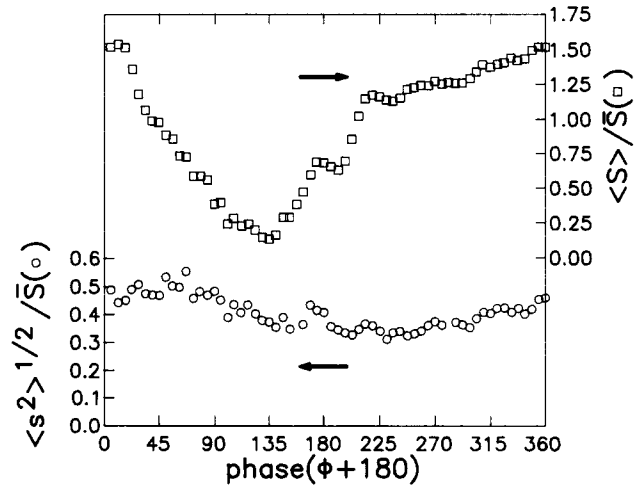

Figure 17. Results from experiment with nonsinusoidal oscillation: $Re = 19{,}300$, $T_o = 1.00$ s; $\bar{S} = 0.94$, $(\bar{s^2})^{1/2} = 0.4$.

As noted in Table 2, the run at $Re = 19{,}200$, $T_o = 3.46$ s shows a value $\bar{S} > 1$, consistent with the measurements at $Re = 9{,}700$. However, the experiments at the large Reynolds number for $T_o = 2.00$, 1.50, 1.00 s show a very different behavior in that the values of $\bar{S}$ are significantly lower. It is, therefore, of interest to examine more closely differences in the behavior at high and low Reynolds numbers.

The runs with $T_o = 2.00$ s at $Re = 19{,}410$ and $Re = 9{,}700$ showed the lowest (0.91) and the highest (1.08) values of $\bar{S}$. The characteristic time constant of the turbulence and the magnitude of P^+ are smaller for larger Reynolds numbers. It is noted that $\langle S \rangle$ responds much more rapidly at low Reynolds numbers to the large changes in the pressure gradient that occur when it changes sign. The reason why drag reduction is associated with the response time of the flow is not understood. No clues to the cause of this drag reduction are obtained from the measurements of $\langle s^2 \rangle^{1/2}$, which seem to be quite similar for the two Reynolds numbers.

Discussion

The main objective of this study was to explore whether large-amplitude imposed oscillations could cause a decrease in drag. Presently available methods for measuring directly the velocity field are not accurate enough to carry out such a study. Consequently, the velocity gradient at the wall was measured with flush-mounted mass-transfer probes. This investigation was made possible by the recent development of techniques involving the use of a sandwich probe and an inverse mass-transfer analysis of digitized data.

The only theory on the influence of large-amplitude oscillations involves the assumption that the time variation is slow enough that a pseudo-steady-state approximation is valid. An increase of the time-averaged drag is indicated.

Experiments with imposed sinusoidal oscillations were carried out at large enough frequencies, $\omega^+ = 0.0138$, 0.0276, 0.0506, that a pseudo-steady-state approximation would not be applicable. Consequently, the measurements of $\bar{S} = 1.01$, 1.00, 1.03, 1.02 for dimensionless $\hat{S}$ of 0.36, 0.57, 0.77, and

1.05 indicate that no change in $\overline{S}$ (or of $\overline{s^2}$) is obtained with large-amplitude sinusoidal imposed oscillations.

However, experiments with $\hat{S}=1.34$ and 1.92, which had flow reversal over an appreciable part of the cycle, showed significant drag reduction. For example, the change of $\hat{S}$ from 0.77 to 1.34 at $\omega^+=0.0276$ caused a change of $\overline{S}$ from 1.03 to 0.95 (8% drag reduction); a change of $\hat{S}$ from 1.05 to 1.92 at $\omega^+=0.0506$ caused a change of $\overline{S}$ from 1.02 to 0.89 (13% drag reduction).

It should be noted that during periods of flow reversal a negative contribution to the drag is being made. (However, energy dissipation very close to the wall was probably not decreased.) Drag reduction would not be found if the probe measurements were not properly analyzed. For example, inconclusive results were obtained during initial studies in our laboratory in which we used pseudo-steady-state methods.

The experiments with nonsinusoidal imposed oscillations were carried out at low frequencies. They were designed to explore whether the phenomenon of drag reduction in the presence of favorable pressure gradients could be exploited. In this sense, the experiments were not successful.

Drag reduction, however, was observed when the Reynolds number was increased from 9,700 to 19,200. The reason is not understood; it seems to be associated with the decrease in the turbulence time scales with increasing flow. This decreases the ability of the flow to respond to sudden changes of the pressure gradient. Within this context, drag reduction occurs because the flow does not respond as rapidly to a rapid change from an unfavorable pressure gradient to a favorable pressure gradient as it does to a rapid change from a favorable pressure gradient to an unfavorable pressure gradient.

Acknowledgment

The authors acknowledge support of this work by the National Science Foundation under Grants NSF CTS 89-19843 and NSF CTS 92-00936.

Literature Cited

Ambari, A., C. Deslouis, and B. Tribollet, "Frequency Response of the Mass Transfer Rate in a Modulated Flow at Electrochemical Probes," *Int. J. Heat Mass Transf.*, **29**, 35 (1986).

Back, L. H., and R. A. Seban, "Convective Heat Transfer in a Convergent-Divergent Nozzle," *Proc. Heat Trans., Fluid Mech. Inst.*, **20**, 410 (1967).

Badri Narayanan, M. A., and V. Ramjee, "On the Criteria for Reverse Transition in a Two-Dimensional Boundary Layer Flow," *J. Fluid Mech.*, **35**, 225 (1969).

Finnicum, D. S., "Pressure Gradient Effects in the Viscous Wall Region of a Turbulent Flow," PhD thesis, Univ. of Illinois at Urbana-Champaign, IL (1986).

Finnicum, D. S., and T. J. Hanratty, "Effect of Favorable Pressure Gradients on Turbulent Boundary Layers," *AIChE J.*, **34**, 529 (1988).

Finnicum, D. S., and T. J. Hanratty, "Influence of Imposed Flow Oscillations on Turbulence," *Physico-Chem. Hydrody.*, **10**, 585 (1988).

Fortuna, G., and T. J. Hanratty, "Frequency Response of the Boundary Layer on Wall Transfer Probes," *Int. J. Heat Mass Transf.*, **14**, 1499 (1971).

Hanratty, T. J., "Use of Polarographic Method to Measure Wall Shear Stress," *J. Appl. Electrochemistry*, **21**, 1038 (1991).

Hanratty, T. J., and J. A. Campbell, "Measurement of Wall Shear Stress," *Fluid Mechanics Measurements*, R. J. Goldstein, ed., Hemisphere, p. 559 (1983).

Hussain, A. K. M. F., and W. C. Reynolds, "The Mechanics of a Perturbation Wave in Turbulent Shear Flow," Stanford Univ. Thermosci. Div. Tech. Rep. FM-6 (1970).

Jones, W. P., and B. E. Launder, "Some Properties of Sink-Flow Turbulent Boundary-Layers," *J. Fluid Mech.*, **56**, 337 (1972).

Kaiping, P., "Unsteady Forced Convective Heat Transfer from a Hot Film in Non-Reversing and Reversing Flow," *Int. J. Heat Mass Transf.*, **26**, 545 (1983).

Mao, Z. X., "Studies of the Wall Shear Stress in a Turbulent Pulsating Pipe Flow," PhD Thesis, Univ. of Illinois at Urbana-Champaign, IL (1984).

Mao, Z., and T. J. Hanratty, "Studies of the Wall Shear Stress in a Turbulent Pulsating Pipe Flow," *J. Fluid Mech.*, **170**, 545 (1986).

Mao, Z., and T. J. Hanratty, "Analysis of Wall Shear Stress Probes in Large Amplitude Unsteady Flows," *Int. J. Heat Mass Transf.*, **34**, 281 (1991a).

Mao, Z., and T. J. Hanratty, "Application of an Inverse Mass Transfer Method to the Measurement of Turbulent Fluctuations in the Velocity Gradient at the Wall," *Exp. in Fluids*, **11**, 65 (1991b).

Mao, Z., and T. J. Hanratty, "Measurement of Wall Shear Stress in Large Amplitude Unsteady Reversing Flows," *Exp. in Fluids*, **12**, 342 (1992).

Mathews, P. M., "The Effect of Large Amplitude Imposed Flow Oscillations in Pipe Flow," MS Thesis, Univ. of Illinois, Urbana-Champaign (1987).

Mitchell, J. E., and T. J. Hanratty, "A Study of Turbulence at a Wall Using an Electrochemical Wall Shear Stress Meter," *J. Fluid Mech.*, **26**, 199 (1966).

Mizushina, T., T. Maruyama, and Y. Shiozaki, "Pulsating Turbulent Flow in a Tube," *J. Chem. Eng. Japan*, **6**, 487 (1973).

Moretti, P. H., and W. M. Kays, "Heat Transfer to a Turbulent Boundary-Layer with Varying Free-Stream Velocity and Varying Surface Temperature—An Experimental Study," *Int. J. Heat Transf.*, **8**, 1187 (1965).

Pedley, T. J., "Heat Transfer from a Hot Film in Reversing Shear Flow," *J. Fluid Mech.*, **78**, 513 (1965).

Py, B., "Etude Tridimensionelle de la sous Couche Visqueuse dans une Veine Rectangulaire par des Mesures de Transfert en Paroi," *Int. J. Heat Mass Transf.*, **15**, 129 (1973).

Ramaprian, B. R., and S. W. Tu, "Fully Developed Periodic Turbulent Pipe Flow," *J. Fluid Mech.*, **137**, 59 (1983).

Ronnenberger, D., and C. D. Ahrens, "Wall Shear Stress Caused by Small Amplitude Perturbations of Turbulent Boundary-Layer Flow: An Experimental Investigation," *J. Fluid Mech.*, **83**, 433 (1977).

Son, J. S., and T. J. Hanratty, "Velocity Gradients at the Wall for Flow around a Cylinder at Reynolds Numbers of 5×10^3 to 10^6," *J. Fluid Mech.*, **35**, 353 (1969).

Tu, S. W., and B. R. Ramaprian, "Fully Developed Periodic Turbulent Pipe Flow: 1. Main Experimental Results and Comparison with Predictions," *J. Fluid Mech.*, **137**, 31 (1983).

Manuscript received June 21, 1993, and revision received Nov. 12, 1993.